Case for polar uranium octupoles in cubic U_2N_3

S. W. Lovesey [*]

ISIS Facility, STFC, Didcot, Oxfordshire OX11 0QX, United Kingdom;
Diamond Light Source, Harwell Science and Innovation Campus, Didcot, Oxfordshire OX11 0DE, United Kingdom;
and Department of Physics, Oxford University, Oxford OX1 3PU, United Kingdom

Uranium ions in the sesquinitride α-U_2N_3 occupy independent acentric and centrosymmetric sites according to conventional x-ray diffraction patterns [R. Troć, J. Solid State Chem. **13**, 14 (1975)]. We submit that polar uranium multipoles in acentric sites are revealed in resonant x-ray diffraction data recently published by Lawrence Bright *et al.* [Phys. Rev. B **100**, 134426 (2019)]. To this end, their diffraction data gathered with a primary x-ray energy in the vicinity of the uranium M_4 absorption edge are compared to symmetry-informed diffraction amplitudes calculated for the bixbyite α-Mn_2O_3 lattice structure. Bragg spots forbidden in this lattice diffraction pattern appear to provide clear-cut evidence for high-order polar uranium multipoles.

I. INTRODUCTION

X-ray diffraction patterns gathered on crystalline materials can contain Bragg spots that do not exist in patterns created by spheres of atomic charge located at points on the particular lattice. Their inherent weakness is off-set by tuning the energy of primary x-rays from a synchrotron source to a specific atomic resonance. The process is often called T & T scattering to acknowledge early experimental studies by Templeton and Templeton [1–5], or anisotropic tensor scattering [6–8]. The weak Bragg spots are not indexed by Miller indices for the lattice symmetry, i.e., they are space-group forbidden. Departures from spheres of atomic charge are usually labeled by components of an electronic quadrupole (multipole rank = 2) that are invariant with respect to operations in the symmetry of sites occupied by the resonant ions (Neumann's Principle [9]). Specifically, acentric sites in a crystal can harbor polar (parity-odd) multipoles.

Following Lawrence Bright *et al.*, we use the bixbyite α-Mn_2O_3-type lattice depicted in Fig. 1, with uranium ions in acentric sites 24d (U2) and centrosymmetric sites 8b (U1) [10,11,12]. The authors mention forbidden reflections (1, 1, 0), (3, 1, 0), and (3, 3, 0), and display data for the (0, 1, 3) Bragg spot, which is equivalent to (3, 1, 0) in cubic bixbyite.

From a historical perspective, it was standard practice to use Cartesian tensors to describe bulk properties of crystals at the time Nye's [13] monograph was published. Spherical electronic tensors (multipoles) in x-ray dichroic signals and diffraction amplitudes can be formulated with Racah

techniques used in atomic physics [14,15]. Example calculations that incorporate sum rules for absorption edges [16] include neptunium and copper multipoles in NpO_2 and CuO [17,18]. Many compounds and the electronic multipoles they harbor have been successfully examined with *ab initio* techniques [19,20]. In our study of space-group forbidden reflections by (cubic) α-U_2N_3, we encounter uranium dipoles (rank = 1), quadrupoles, and octupoles (rank = 3) that must be present in a meaningful model of the electronic structure. By way of an example of the high value of information that can be extracted from the intensity of a space-group forbidden Bragg spot, we mention resonant x-ray diffraction by TbB_4 [21]. An observed coupling of such intensity with helicity (circular polarization) in the primary x-ray beam implies that the crystal class of TbB_4 is not a conventional one mentioned by the authors [21]. Instead, the available evidence is that TbB_4 and an altermagnet possess similar symmetries [22].

II. LATTICE STRUCTURE

Space group $Ia\bar{3}$ (No. 206) describes the (cubic) bixbyite α-Mn_2O_3-type lattice [10]. (We use the Belov-Neronova-Smirnova (BNS) setting of space groups, and the Bilbao Crystallographic Server [23].) A body-centered translation requires that integer Miller indices h, k, l have an even sum. Equivalent reflections for No. 206 are listed in Appendix A. A magnetic diffraction pattern observed below $T_N \approx 73.5$ K is consistent with an antitranslation and odd $(h + k + l)$ [12]. The measured lattice constant $a \approx 10.69$ Å (this is one of two values cited in Ref. [12]).

Lawrence Bright *et al.* [12] made measurements on thin epitaxial films of U_2N_3 grown on CaF_2 substrates ($a_0 = 5.451$ Å). The lattice parameter in the direction of growth was 10.80(1) Å, compared to $2a_0$ (CaF_2) = 10.9 Å, and the in-plane parameters were 10.60(2) Å. The implication is that for their thin films, where the mosaicity is low, the symmetry is metrically orthorhombic and not cubic. For thicker films
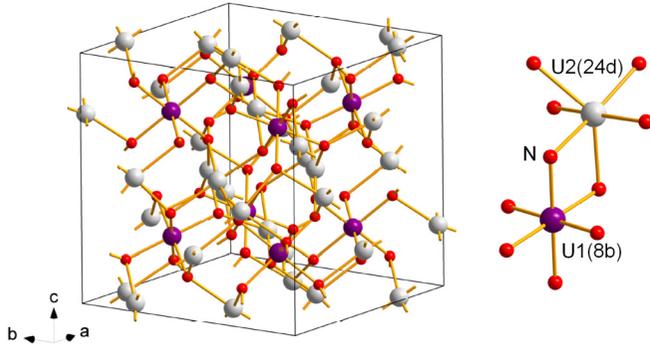
_____

[*] stephen.lovesey@stfc.ac.uk

FIG. 1. The bixbyite structure No. 206 has sixfold coordinated cations (large spheres) occupying centrosymmetric 8b (U1) and acentric 24d (U2) Wyckoff sites [23]. Cation sites are surrounded by local octahedra with oxygen (small spheres) at their vertexes.

where the mosaicity is larger, this might mean the induced orthorhombic strain has been relaxed and the bulk of a film is cubic. Diffraction by an appropriate orthorhombic lattice symmetry appears in Sec. V, and we continue to study diffraction by uranium ions in cubic $Ia\bar{3}$ (No. 206).

III. RESONANT X-RAY DIFFRACTION

States of x-ray polarization, Bragg angle θ, and the plane of scattering are shown in Fig. 2. The x-ray scattering length in the unrotated channel of polarization $\sigma \to \sigma'$, say, is modeled by $(\sigma'\sigma)/D(E)$. In this instance, the resonant denominator is replaced by a sharp oscillator $D(E) = [(E - \Delta + i\Gamma/2)/\Delta]$, with the x-ray energy E in the near vicinity of an atomic resonance Δ of total width Γ, namely, $E \approx \Delta$ and $\Gamma \ll \Delta$ [24]. The cited energy-integrated scattering amplitude $(\sigma'\sigma)$, one of four amplitudes, is studied using standard tools and methods from atomic physics and crystallography. Resonant processes from M edges utilize atomic states $3d$ to $5f$ (electric dipole, E1) and $3d$ to $7s$, $6d$ (electric quadrupole, E2). The meaningful comparison of E1 and E2 radial integrals in
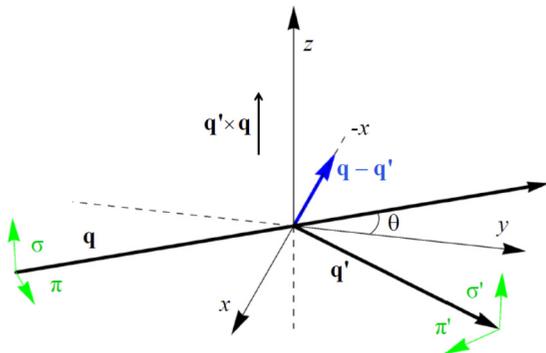

FIG. 2. Primary (σ, π) and secondary (σ', π') states of x-ray polarization. Corresponding wavevectors **q** and **q**′ subtend an angle 2θ. The Bragg condition for diffraction is met when $\mathbf{q} - \mathbf{q}'$ coincides with a reflection vector (h, k, l). Crystal vectors in Fig. 1 and the depicted Cartesian (x, y, z) coincide in the nominal setting of the crystal, and the start $\psi = 0$ of an azimuthal angle scan (rotation of the crystal by an angle ψ about the reflection vector).

diffraction amplitudes includes the photon wavelength λ in E2 [24]. In the present case, $(3d|R|5f)$ should be compared with $[(2\pi/\lambda)(3d|R^2|7s)]$ or $[(2\pi/\lambda)(3d|R^2|6d)]$. One finds the dimensionally correct E2 integrals are a factor ≈ 16 smaller than the standard E1 radial integral $(3d|R|5f)$ for $\lambda \approx 3.33$ Å (based on $\Delta \approx 3.73$ keV). An E1-E1 (E1-E2) scattering event is parity even (parity odd) and exposes axial (polar) electronic properties.

In our adopted description of electronic degrees of freedom, uranium ions are assigned spherical multipoles $\langle O_Q^K \rangle$ of integer rank K with projections Q in the interval $-K \leqslant Q \leqslant K$. Multipoles obey sum rules that relate values evaluated at absorption events labeled by the core spin-orbit interaction [16,18,24]. A unit-cell electronic structure factor Ψ_Q^K is compiled from all symmetry operations for uranium ions in space group No. 206 [23]. An axial structure factor, with a parity signature $\sigma_\pi = +1$ in Eq. (A3), say, defines space-group forbidden reflections. For these reflections, an axial Ψ_Q^K is zero with $Q = 0$ and even K. Previously published axial and polar Ψ_Q^K include results suitable for the compounds GdB$_4$, Cr$_2$O$_3$, LaMnO$_3$, NpO$_2$, and CuO [17,18,24]. Our Ψ_Q^K (24d) and Ψ_Q^K (8b) are reported in Appendix A. The main text of this work is given over to a discussion of key implications for weak (space-group forbidden) Bragg spots available from resonant x-ray Bragg diffraction.

Cartesian and spherical components $Q = 0, \pm1$ of a vector $\mathbf{n} = (\xi, \eta, \zeta)$ are related by $\xi = (n_{-1} - n_{+1})/\sqrt{2}$, $\eta = i(n_{-1} + n_{+1})/\sqrt{2}$, $\zeta = n_0$. A complex conjugate of a multipole is defined as $\langle O_Q^K \rangle^* = (-1)^Q \langle O_{-Q}^K \rangle$, meaning the diagonal multipole $\langle O_0^K \rangle$ is purely real. The phase convention for real and imaginary parts labeled by single and double primes is $\langle O_Q^K \rangle = [\langle O_Q^K \rangle' + i\langle O_Q^K \rangle'']$. Whereupon, Cartesian dipoles are $\langle O_\xi^1 \rangle = -\sqrt{2}\langle O_{+1}^1 \rangle'$ and $\langle O_\eta^1 \rangle = -\sqrt{2}\langle O_{+1}^1 \rangle''$.

IV. WEAK REFLECTIONS: CUBIC $Ia\bar{3}$

We consider a Bragg reflection vector $(h, k, 0)$ with even $(h + k)$ in keeping with Table I in Ref. [12]. Odd integer Miller indices h and k produce space-group forbidden reflections, e.g., Ψ_Q^K (8b) $= 0$ for the projection $Q = 0$ with even K, and $(1, 1, 0)$, $(3, 1, 0)$, and $(3, 3, 0)$ are specifically mentioned [12]. The electronic structure factor [Eq. (A2)] for Ψ_Q^K (8b) can different from zero for odd Q, however. Axial multipoles have an even rank and $K = 2$ in an E1-E1 absorption event [25]. Since the quadrupoles $\langle T_{\pm1}^2 \rangle_b$ are not invariant with respect to $3_{xyz}^\pm$ in the full 8b site symmetry, uranium ions in the centrosymmetric sites do not contribute to the defined pattern of weak Bragg spots. We continue the discussion of weak Bragg spots with diffraction by uranium ions in acentric 24d sites.

Evaluated for $(h, k, 0)$, the electronic structure factor [Eq. (A3)] for Ψ_Q^K (24d) reduces to

$$\Psi_Q^K(24\text{d}) = \langle O_Q^K \rangle_d [\alpha(h) + \alpha(h)^* \sigma_\pi][1 - (-1)^Q \sigma_\pi]$$
$$+ 2\alpha(k)'\gamma(h)3_{xyz}^+ \langle O_Q^K \rangle_d [1 - \sigma_\pi]$$
$$(2n + 1, 2m + 1, 0). \quad (1)$$

Spatial phase factors are $\alpha(h) = \exp(i2\pi hx)$, with $x \approx -0.02$ [12], and $\gamma(h) = \exp(i\pi h/2)$. Notably, multipoles $3_{xyz}^+ \langle O_Q^K \rangle_d$

are wholly absent in Eq. (1), and axial $3^+_{xyz} \langle T^K_Q \rangle_d$ with parity signature $\sigma_\pi = +1$ are absent.

Universal results for diffraction amplitudes are listed in Ref. [25] as functions of two electronic quantities, even and odd, with respect to the sign of projections Q, namely, $A^K_{-Q} = A^K_Q$ and $B^K_{-Q} = -B^K_Q$. They are functions of the azimuthal angle ψ (angle of rotation of the crystal about the reflection vector), with the crystal c-axis normal to the plane of scattering at the beginning of a scan $\psi = 0$. For the case in hand [equivalent reflections for space group $Ia\bar{3}$ (No. 206) are listed in Appendix A],

$$A^K_Q + B^K_Q = \mathrm{e}^{(iQ\chi)} \Psi^K_Q, \quad (h, k, 0) \tag{2}$$

where $\cos(\chi) = -h/\sqrt{[h^2 + k^2]}$.

Axial multipoles ($\sigma_\pi = +1$) contribute standard T & T scattering proportional to the uranium quadrupole $\langle T^2_Q \rangle_d$ with odd Q [1–5]. The E1-E1 amplitude $(\sigma'\sigma)_{11}$ is purely real,

$$(\sigma'\sigma)_{11} = \cos(\chi) \sin(2\psi) \alpha(h)' \langle T^2_{+1} \rangle''_d, \quad (h, k, 0), \tag{3}$$

with $\alpha(h)' = \cos(2\pi hx)$. The diffraction amplitude in which x-ray polarization is rotated from σ to π' contains an additional contribution [25],

$$(\pi'\sigma)_{11} = \alpha(h)' \langle T^2_{+1} \rangle''_d [\sin(\theta) \cos(\chi) \cos(2\psi)$$
$$+ \cos(\theta) \sin(\chi) \cos(\psi)], \quad (h, k, 0), \tag{4}$$

and $(\sigma'\pi)_{11}$ is obtained by changing the sign of the Bragg angle θ.

Uranium polar multipoles ($\sigma_\pi = -1$) are denoted $\langle U^K_Q \rangle$ [18,24], and we henceforth safely drop the subscript d given that they are exclusive to 24d. It is convenient to write the E1-E2 amplitude $(\sigma'\sigma)_{12}$ as a sum of two parts, one proportional to $\alpha(h)''$ (labeled V) and one proportional to $\alpha_k(k)'$ (labeled W), i.e., $(\sigma'\sigma)_{12} = V + [\gamma(h)W]$. The amplitude $(\sigma'\sigma)_{12}$ depends on the Bragg angle, unlike $(\sigma'\sigma)_{11}$. We find V is a sum of multipoles with even projections, two quadrupoles (rank $K = 2$), and an octupole (rank $K = 3$) [25],

$$V = (1/\sqrt{30})\alpha(h)'' \sin(\theta) \sin(2\psi) \left[\sqrt{(3/2)} \langle U^2_0 \rangle \right.$$
$$\left. + \cos(2\chi)\{ \langle U^2_{+2} \rangle' + 2\sqrt{2} \langle U^3_{+2} \rangle'' \} \right], \quad (h, k, 0). \tag{5}$$

There are seven purely imaginary contributions to W, which is proportional to $\sin(\theta)$. The factor $\gamma(h) = \exp(i\pi h/2)$ renders $[\gamma(h)W]$ in $(\sigma'\sigma)_{12}$ real for odd h. An actual expression for W can be read off from Eq. (D1) in Ref. [25] by inserting multipoles listed in Appendix A to this work. For the special case $\cos(2\chi) = 0$ and $h = 2n + 1$,

$$(\sigma'\sigma)_{12} = \sin(\theta) \left[(1/\sqrt{20}) \alpha(h)'' \sin(2\psi) \langle U^2_0 \rangle \right.$$
$$- (i/5) \sqrt{6}\gamma(h) \alpha(h)'$$
$$\times \{ \hat{E}^1_1 + (1/2)\sqrt{(5/6)} \sin(2\psi) \hat{A}^2_0$$
$$+ (i/3) \sqrt{5} \cos(2\psi)\hat{A}^2_1 + (1/6) [5 \cos(2\psi) + 3]$$
$$\times \hat{E}^3_1 - \sqrt{(5/3)}\sin^2(\psi)\hat{E}^3_3 \} \right]$$
$$(2n + 1, 2n + 1, 0). \tag{6}$$

Polar dipoles, quadrupoles, and octupoles $\hat{E}^1_1$, $\hat{A}^2_Q$, $\hat{E}^3_Q$ appearing in Eq. (6) are listed in Eq. (A6). In summary, the dependence of $(\sigma'\sigma)_{12}$ on ψ is a linear combination of

$\cos(2\psi)$ and $\sin(2\psi)$ on a background set by a dipole $\hat{E}^1_1$ directed along the a-axis in Fig. 1.

By way of a contrast to forbidden reflections considered thus far in our work, we give an amplitude for reflection vectors $(2n, 0, 0)$ parallel to a dyad axis of rotation symmetry. It is classified as a weak reflection in Table I of Ref. [12]. Diffraction by uranium ions 8b are allowed using axial events E1-E1 or E2-E2. The unrotated polar amplitude is

$$(\sigma'\sigma)_{12} = (4/5)\sqrt{6}\,\alpha(h)'' \sin(\theta)[\langle U^1_{+1} \rangle'$$
$$- (1/3)\sqrt{5} \cos(2\psi)\langle U^2_{+1} \rangle'' + (1/6)$$
$$\times [5 \cos(2\psi) + 3]\langle U^3_{+1} \rangle' - \sqrt{(5/3)} \sin^2(\psi)\langle U^3_{+3} \rangle']$$
$$(2n, 0, 0), \tag{7}$$

with the crystal c-axis is normal to the plane of scattering for $\psi = 0$. The amplitude $(\sigma'\sigma)_{12}$ is an even function of the azimuthal angle, namely, $\cos(2\psi)$, unlike the result for $(2n + 1, 2n + 1, 0)$, which has a lower symmetry with respect to crystal axes. The dyad imposes twofold symmetry in ψ.

V. REDUCED LATTICE SYMMETRY: *Ibca*

The parent cubic space group $Ia\bar{3}$ (No. 206) does not contain any fourfold axes. In consequence, a strained film can only be orthorhombic. If we take into account the orthorhombic macroscopic strains (imposed by the misfit with the substrate), the reduced symmetry is orthorhombic *Ibca* (No. 73), which keeps the lattice vectors and origin of the parent structure and origin. This lattice symmetry still forbids $(3, 1, 0)$ or any other reflection $(h, k, 0)$ with odd h, k. Electronic structure factors for uranium ions are given in Appendix B. An accompanying list of equivalent reflections confirms that $(3, 1, 0)$ and $(1, 3, 0)$ are not equivalent in the orthorhombic space group. To begin with, we compare some forbidden $(h, k, 0)$ scattering amplitudes with foregoing results derived for the cubic space group $Ia\bar{3}$.

Uranium ions in sites 8b contribute diffraction enhanced by an E1-E1 event, whereas special sites do not contribute in the cubic lattice. Axial T & T scattering with odd h and k include

$$(\sigma'\sigma)_{11} = \sin(\chi) \sin(2\psi)\langle T^2_{+1} \rangle'_b, \quad (2n + 1, 2m + 1, 0), \tag{8}$$

$$(\pi'\sigma)_{11} = \langle T^2_{+1} \rangle'_b [\sin(\theta) \sin(\chi) \cos(2\psi)$$
$$- \cos(\theta) \cos(\chi) \cos(\psi)]. \tag{9}$$

The amplitude $(\sigma'\pi)_{11}$ is obtained from Eq. (9) by a change in sign of the Bragg angle θ. Contributions to T & T scattering in $(\sigma'\sigma)_{11}$ from sites 8c and 8d are proportional to $\sin(2\psi)$, as in Eq. (8). The remaining factors in $(\sigma'\sigma)_{11}$ for the two sites are $[\alpha(h)' \cos(\chi)\langle T^2_{+1} \rangle''_c]$ and $[i\alpha''(k)\gamma(h) \sin(\chi)\langle T^2_{+1} \rangle'_d]$.

The polar amplitude $(\sigma'\sigma)_{12}$ for sites 8c is also proportional to $\sin(2\psi)$. A uranium octupole $\langle U^3_{+2} \rangle''_c$ is engaged:

$$(\sigma'\sigma)_{12} = (1/\sqrt{20}) \sin(\theta) \alpha(h)'' \sin(2\psi)$$
$$\times [\langle U^2_0 \rangle_c + \cos(2\chi) \sqrt{(2/3)}\langle U^2_{+2} \rangle'_c$$
$$+ (4/\sqrt{3})\langle U^3_{+2} \rangle''_c], \quad (2n + 1, 2m + 1, 0). \tag{10}$$

The corresponding result for sites 8d is obtained by the substitution $\alpha(h)'' \to -i\alpha(k)' \gamma(h)$ along with $\langle U_Q^K \rangle_c \to \langle U_Q^K \rangle_d$. The octupole is a greater presence in the rotated channel, for which we find

$$(\pi'\sigma)_{12}$$

$$= \text{polar quadrupoles} + (2/\sqrt{15}) \sin(\theta) \alpha(h)'' \langle U_{+2}^3 \rangle_c''$$

$$\times [\cos(\theta) \sin(2\chi) \cos(\psi) + \sin(\theta) \cos(2\chi) \cos(2\psi)],$$

$$(2n+1, 2m+1, 0), \qquad (11)$$

with a similar result for sites 8d.

Turning to site 8e, the electronic structure factor [Eq. (B3)] is zero for $\sigma_\pi = +1$ using odd k and $l = 0$. The polar amplitude $(\sigma'\sigma)_{12}$ can be different from zero, however, and an octupole is engaged. We find

$$(\sigma'\sigma)_{12} = (i/\sqrt{30}) \sin(\theta) \alpha(h)'' \gamma(k) \sin(2\psi) \sin(2\chi)$$

$$\times [\langle U_{+2}^2 \rangle_e'' - (4/\sqrt{3})\langle U_{+2}^3 \rangle_e'],$$

$$(2n+1, 2m+1, 0). \qquad (12)$$

There is not scope from the azimuthal angle dependences of $(\sigma'\sigma)_{12}$ to differentiated between sites. However, for site 8e, $(\sigma'\sigma)_{12} = 0$ for $\chi = 0$, while contributions are allowed from 8c and 8d for this reflection vector.

Diffraction amplitudes for reflections $(0, k, l)$ with even $(k + l)$ and odd k can be derived starting from Eq. (B4). Axial amplitudes for the special sites 8b are absent, namely, $(\sigma'\sigma)_{11} = (\pi'\sigma)_{11} = 0$. The electronic structure factor $\Psi_Q^K(8c)$ in Eq. (B1) vanishes for axial multipoles with $\sigma_\pi = +1$, while $(\sigma'\sigma)_{12} \propto \sin(2\chi)$ with $\cos(\chi) = k/\sqrt{[k^2 + l^2]}$. Axial T & T scattering by uranium ions in general sites 8d and 8e is performed by quadrupoles $\langle T_{+1}^2 \rangle_d'$ and $\langle T_{+2}^2 \rangle_e''$, respectively. Polar multipoles $(\sigma_\pi = -1)$ that arise in the unrotated channel $(\sigma'\sigma)_{12}$ are similar for the two sites. Specifically, $(\sigma'\sigma)_{12}$ contains a contribution from an octupole $\propto [\cos(2\chi)\langle U_{+2}^3 \rangle'']$.

VI. CONCLUSION

It is argued that the observation of a space-group forbidden Bragg spot in resonant x-ray diffraction by cubic U_2N_3 is solid evidence of uranium electronic multipoles in the material [8,12,26,27]. Multipoles include a dipole parallel to the crystal a-axis, and octupoles. Such results take our case beyond axial quadrupoles engaged in conventional Templeton-Templeton scattering, as in Eqs. (3) and (4) [1–5]. Looking ahead, our predicted azimuthal angle scans, intensity versus rotation of the sample about the reflection vector, need testing. The outcome could sway a debate about the relevant significance of axial and polar uranium multipoles in cubic U_2N_3, as we see in Eqs. (3) and (6) for diffraction amplitudes $(\sigma'\sigma)_{11}$ and $(\sigma'\sigma)_{12}$.

Electronic structure factors [Eqs. (A2) and (A3)] for uranium ions have been used mainly to interpret resonant x-ray diffraction in the unrotated channel of polarization $(\sigma'\sigma)$ [12]. Universal expressions for all four amplitudes in Ref. [25] permit an exhaustive investigation at the time data are available, using electric dipole-electric dipole (E1-E1), electric dipole-electric quadrupole (E1-E2) or E2-E2 absorption events. For

the moment, we have used E1-E1 and E1-E2, and included a few statements about the rotated channel $(\pi'\sigma)$. Beyond resonant x-ray diffraction, structure factors [Eqs. (A2) and (A3)] can be used to calculate neutron diffraction patterns [28].

Our theoretical investigation is motivated by diffraction patterns collected from thin epitaxial films of U_2N_3 [12]. Lawrence Bright *et al.* [12] report in-plane lattice parameters that are different from the growth directions. This piece of information plants the idea that the lattice symmetry for the diffraction patterns of interest is metrically orthorhombic and not cubic, an idea we pursue in Sec. V and Appendix B.

APPENDIX A: CUBIC $Ia\bar{3}$ (NO. 206)

An electronic structure factor is

$$\Psi_Q^K = [\exp(i\kappa \cdot \mathbf{e})\langle O_Q^K \rangle_e], \qquad (A1)$$

where the reflection vector $\kappa = (h, k, l)$ and the implied sum is over resonant ions in the unit cell at positions $\mathbf{e}$. Values of Ψ_Q^K suitable for GdB_4, Cr_2O_3, $LaMnO_3$, NpO_2, and CuO, for example, are found in Refs. [17,18,24].

Returning to U_2N_3, sites 8b in space group No. 206 (crystal class $m\bar{3}$) are centrosymmetric (Fig. 1), and axial multipoles are denoted by $\langle T_Q^K \rangle_b$ [24]. Additional site symmetries for 8b require $\langle T_Q^K \rangle_b$ to be invariant with respect to angular rotations 3_{xyz}^+ and 3_{xyz}^-. We find [23],

$$\Psi_Q^K(8b) = e^{i\pi(h+k+l)/2}[1 + (-1)^h(-1)^Q]$$

$$\times [\langle T_Q^K \rangle_b + (-1)^k(-1)^K\langle T_{-Q}^K \rangle_b]. \qquad (A2)$$

Sites 24d possess symmetry 2_x, and $2_x\langle O_Q^K \rangle_d = (-1)^K\langle O_{-Q}^K \rangle_d = (-1)^{K+Q}\langle O_Q^K \rangle_d^*$ [13]. Thus, a generic multipole $\langle O_Q^K \rangle_d$ is purely real (imaginary) for even (odd) $K + Q$. Spatial phase factors in $\Psi_Q^K(24d)$ include $\alpha(h) = \exp(i2\pi hx)$, $\gamma(h) = \exp(i\pi h/2)$, etc., with $x \approx -0.02$ [12]. A parity signature $\sigma_\pi = +1(-1)$ for axial (polar) multipoles. After tedious algebra,

$$\Psi_Q^K(24d) = \gamma(l)\langle O_Q^K \rangle_d[\alpha(h) + (-1)^l\alpha(h)^*\sigma_\pi]$$

$$\times [1 + (-1)^h(-1)^Q\sigma_\pi] + \gamma(h)3_{xyz}^+\langle O_Q^K \rangle_d$$

$$\times [\alpha(k) + (-1)^l\alpha(k)^*][1 + (-1)^k\sigma_\pi]$$

$$+ \gamma(k)3_{xyz}^-\langle O_Q^K \rangle_d[\alpha(l) + (-1)^h\alpha(l)^*]$$

$$\times [1 + (-1)^l\sigma_\pi]. \qquad (A3)$$

A derivation of $\Psi_Q^K(24d)$ exploits the identities $3_{xyz}^+(x, y, z) = (z, x, y) = 2_x3_{-xy-z}^+(x, y, z)$, and $3_{xyz}^-(x, y, z) = (y, z, x) =$

$2_x 3^-_{-x-yz}(x, y, z)$, which can be derived from tables in Appendix 1 of Ref. [31]. In the unrealistic case of identical uranium ions at the two independent sites, $[\Psi_0^K(8b) + \Psi_0^K(24d)] = 0$ for even K, $(h, h, 0)$, $\gamma(h) = -1$, and $\sigma_\pi = +1$. Multipoles $3^\pm_{xyz}\langle O_Q^K \rangle$ in Eq. (A3) can be constructed from

$$3^+_{xyz}\langle O_Q^K \rangle = \exp(iq\beta)d_{Qq}^K(\beta)\langle O_q^K \rangle, \quad \text{(A4)}$$

$$3^-_{xyz}\langle O_Q^K \rangle = \exp(iQ\beta)(-1)^q d_{Qq}^K(\beta)\langle O_q^K \rangle, \quad \text{(A5)}$$

with a sum on projections q, and $d_{Qq}^K(\beta)$ is a standard Wigner rotation matrix with an argument $\beta = \pi/2$ [32]. The identity $d_{-Qq}^K(\beta) = (-1)^{K+q}d_{Qq}^K(\beta)$ is useful in calculations.

We list multipoles exposed at a reflection $(2n + 1, 2m + 1, 0)$ with $\cos(\chi) = -h/\sqrt{[h^2 + k^2]}$. Polar $(\sigma_\pi = -1)$ uranium multipoles in W are defined by $(\sigma'\sigma)_{12} = [V + \gamma(h)W]$, and they are

$$\begin{aligned}
\hat{E}_1^1 &= -\sin(\chi)\langle U_{+1}^1 \rangle' = \sin(\chi)\langle U_a^1 \rangle/\sqrt{2}, \\
\hat{A}_2^2 &= (1/2)\cos(2\chi)[\sqrt{(3/2)}\langle U_0^2 \rangle - \langle U_{+2}^2 \rangle'], \\
\hat{A}_1^2 &= i\sin(\chi)\langle U_{+1}^2 \rangle'', \\
\hat{A}_0^2 &= -[(1/2)\langle U_0^2 \rangle + \sqrt{(3/2)}\langle U_{+2}^2 \rangle'], \\
\hat{E}_3^3 &= (1/4)\sin(3\chi)[-\sqrt{15}\langle U_{+1}^3 \rangle' + \langle U_{+3}^3 \rangle'], \\
\hat{E}_2^3 &= i\cos(2\chi)\langle U_{+2}^3 \rangle'', \\
\hat{E}_1^3 &= (1/4)\sin(\chi)[\langle U_{+1}^3 \rangle' + \sqrt{15}\langle U_{+3}^3 \rangle']. \quad \text{(A6)}
\end{aligned}$$

Space group: equivalent reflections for cubic No. 206:

(1)h, k, l; (2) $-h, -k, l$; (3) $-h, k, -l$; (4)$h, -k, -l$;

(5)l, h, k; (6)$l, -h, -k$; (7) $-l, -h, k$;

(8) $-l, h, -k$; (9)k, l, h; (10) $-k, l, -h$;

(11)$k, -l, -h$; (12) $-k, -l, h$; (13) $-h, -k, -l$;

(14)$h, k, -l$; (15)$h, -k, l$; (16) $-h, k, l$;

(17) $-l, -h, -k$; (18) $-l, h, k$; (19)$l, h, -k$; (20)$l, -h, k$;

(21) $-k, -l, -h$; (22)$k, -l, h$; (23) $-k, l, h$; (24)$k, l, -h$. (A7)

APPENDIX B: ORTHORHOMBIC *Ibca* (NO. 73)

Miller indices h, k, l have an even sum for space group *Ibca* (No. 73, crystal class *mmm*). Uranium ions occupy four independent sites, one special (8b) and three general (8c, 8d, 8e) [10,23]. The electronic structure factor $\Psi_Q^K(8b)$ is identical to Eq. (A2), with site symmetry reduced from $\bar{3}$ in No. 206 to inversion alone in No. 73. The remaining three electronic structure factors are

$$\begin{aligned}
\Psi_Q^K(8c) &= \gamma(l)\langle O_Q^K \rangle_c[\alpha(h) + (-1)^l\alpha(h)^*\sigma_\pi] \\
&\times [1 + (-1)^h(-1)^Q\sigma_\pi], \quad \text{(B1)}
\end{aligned}$$

$$\begin{aligned}
\Psi_Q^K(8d) &= \gamma(h)\langle O_Q^K \rangle_d[\alpha(k) + (-1)^h\alpha(k)^*\sigma_\pi] \\
&\times [1 + (-1)^k(-1)^Q\sigma_\pi], \quad \text{(B2)}
\end{aligned}$$

$$\begin{aligned}
\Psi_Q^K(8e) &= \gamma(k)\langle O_Q^K \rangle_c[\alpha(l) + (-1)^k\alpha(l)^*\sigma_\pi] \\
&\times [\langle O_Q^K \rangle_e + (-1)^l(-1)^K\sigma_\pi\langle O_{-Q}^K \rangle_e]. \quad \text{(B3)}
\end{aligned}$$

Sites symmetries in Eqs. (B1), (B2) and (B3) are 2_x (8c), 2_y (8d), and 2_z (8e), leading to $\langle O_Q^K \rangle_{c^*} = (-1)^{K+Q}\langle O_Q^K \rangle_c$, $\langle O_Q^K \rangle_{d^*} = (-1)^K\langle O_Q^K \rangle_d$, and even Q (8e). The general coordinate in a spatial factor $\alpha(h) = \exp(i2\pi hy)$, say, is not known. Data for bixbyite α-Mn_2O_3 suggest $y \approx -0.035$ [10].

Scattering amplitudes for reflections $(0, k, l)$ with even $(k + l)$ and odd k can be derived from

$$A_Q^K + B_Q^K = \gamma(Q)e^{(iQ\chi)}d_{Qq}^K(\beta)\Psi_q^K (0, k, l), \quad \text{(B4)}$$

with a sum on projections q. In the present case, $\cos(\chi) = k/\sqrt{[k^2 + l^2]}$, $\beta = \pi/2$, and $\gamma(Q) = \exp(i\pi Q/2)$, as before. The crystal a-axis is parallel to $-z$ in Fig. 2 at the start of an azimuthal angle scan $\psi = 0$.

Space group: equivalent reflections for orthorhombic No. 73:

(1)h, k, l; (2) $-h, -k, l$; (3) $-h, k, -l$; (4)$h, -k, -l$;
(5) $-h, -k, -l$; (6)$h, k, -l$; (7)$h, -k, l$; (8) $-h, k, l$. (B5)

[1] D. H. Templeton and L. K. Templeton, Acta Crystallogr. A **36**, 237 (1980).

[2] D. H. Templeton and L. K. Templeton, Acta Crystallogr. A **38**, 62 (1982).

[3] D. H. Templeton and L. K. Templeton, Acta Crystallogr. A **41**, 133 (1985).

[4] D. H. Templeton and L. K. Templeton, Acta Crystallogr. A **42**, 478 (1986).

[5] D. H. Templeton, in *Handbook on Synchrotron Radiation*, edited by G. Brown and D. E. Moncton (Elsevier Science, New York, 1991), Vol. 3.

[6] V. E. Dmitrienko, Acta Crystallogr. A **39**, 29 (1983).

[7] V. E. Dmitrienko, K. Ishida, A. Kirfel, and E. N. Ovchinnikova, Acta Crystallogr. A **61**, 481 (2005).

[8] J. Kokubun and V. E. Dmitrienko, Eur. Phys. J. Special Topics **208**, 39 (2012).

[9] F. E. Neumann, *Vorlesungen über die Theorie Elasticität der festen Körper und des Lichtäthers* (Teubner, Leipzig, 1885); A. P. Cracknell, *Magnetism in Crystalline Materials* (Pergamon Press, Oxford, 1975).

[10] A. Fert, Bull. Soc. Francaise Mineral. Cristallogr. **85**, 267 (1962).

[11] R. Troć, J. Solid State Chem. **13**, 14 (1975).

[12] E. L. Bright, R. Springell, D. G. Porter, S. P. Collins, and G. H. Lander, Phys. Rev. B **100**, 134426 (2019).

[13] J. F. Nye, *Physical Properties of Crystals* (Oxford University Press, London, 1964).

[14] J. Luo, G.T. Trammell, and J.P. Hannon, Phys. Rev. Lett. **71**, 287 (1993).

[15] S. W. Lovesey and E. Balcar, J. Phys.: Condens. Matter **8**, 10983 (1996).

[16] B. T. Thole, P. Carra, F. Sette, and G. van der Laan, Phys. Rev. Lett. **68**, 1943 (1992); P. Carra, B. T. Thole, M. Altarelli, and X. D. Wang, *ibid.* **70**, 694 (1993); P. Carra, H. König, B. T. Thole, and M. Altarelli, Physica B **192**, 182 (1993).

[17] S. W. Lovesey, C. Detlefs, and A. Rodríguez-Fernández, J. Phys.: Condens. Matter **24**, 256009 (2012).

[18] S. W. Lovesey and E. Balcar, J. Phys. Soc. Jpn. **82**, 021008 (2013).

[19] M.- T. Suzuki, H. Ikeda, and P. M. Oppeneer, J. Phys. Soc. Jpn. **87**, 041008 (2018).

[20] O. Bunău, A. Y. Ramos, and Y. Joly, *International Tables for Crystallography*, *X-ray Absorption Spectroscopy and Related Techniques* (Wiley, New York, 2022), Vol. I.

[21] R. Misawa, K. Arakawa, T. Yoshioka, H. Ueda, F. Iga, K. Tamasaku, Y. Tanaka, and T. Kimura, Phys. Rev. B **108**, 134433 (2023).

[22] L. Šmejkal, J. Sinova, and T. Jungwirth, Phys. Rev. X **12**, 040501 (2022).

[23] Bilbao Crystallographic Server, http://www.cryst.ehu.es.

[24] S. W. Lovesey, E. Balcar, K. S. Knight, and J. Fernández Rodríguez, Phys. Rep. **411**, 233 (2005).

[25] V. Scagnoli and S. W. Lovesey, Phys. Rev. B **79**, 035111 (2009).

[26] C. Vettier, J. Electron Spectrosc. Relat. Phenomena **117–118**, 113 (2001).

[27] L. Paolasini, Soc. Française Neutronique (SFN) **13**, 03002 (2014).

[28] S. W. Lovesey, Phys. Scr. **90**, 108011 (2015).

[29] R. D. Cowan, J. Opt. Soc. Am. **58**, 808 (1968).

[30] R. D. Cowan, *The Theory of Atomic Structure and Spectra* (University of California Press, Berkeley, 1981).

[31] G. Burns and A. M. Glazer, *Space Groups for Solid State Scientists*, 2nd ed. (Academic Press, Boston, 1990).

[32] A. R. Edmonds, *Angular Momentum in Quantum Mechanics* (Princeton University Press, Princeton, 1960).